1-2007

An Electrostatic/Hydrogen Bond Switch as Basis For the Specific Interaction of Phosphatidic Acid With Proteins

Edgar E. Kooijman
Kent State University - Kent Campus, ekooijma@kent.edu

D. Peter Tieleman
University of Calgary

Christa Testerink
University of Amsterdam

Teun Munnik
University of Amsterdam

Dirk T. S. Rijkers
Utrecht University

See next page for additional authors

Authors
Edgar E. Kooijman, D. Peter Tieleman, Christa Testerink, Teun Munnik, Dirk T. S. Rijkers, and Ben de Kruijff

THE JOURNAL OF BIOLOGICAL CHEMISTRY VOL. 282, NO. 15, pp. 11356–11364, April 13, 2007

An Electrostatic/Hydrogen Bond Switch as the Basis for the Specific Interaction of Phosphatidic Acid with Proteins*[S]

Received for publication, October 16, 2006, and in revised form, January 16, 2007 Published, JBC Papers in Press, February 3, 2007, DOI 10.1074/jbc.M609737200

Edgar E. Kooijman[‡1,2], D. Peter Tieleman[§3], Christa Testerink[¶4], Teun Munnik[¶5], Dirk T. S. Rijkers[‖], Koert N. J. Burger[2,6], and Ben de Kruijff[‡2]**

From the [‡]Department Biochemistry of Membranes, Bijvoet Center, Institute of Biomembranes, Utrecht University, Utrecht 3584 CH, The Netherlands, [§]Department of Biological Sciences, University of Calgary, AB T2N 1N4, Canada, [¶]Section of Plant Physiology, Swammerdam Institute for Life Sciences, University of Amsterdam, Amsterdam 1098 SM, The Netherlands, [‖]Department of Medicinal Chemistry, Utrecht University, Utrecht 3584 CA, The Netherlands, and [**]Department of Biochemical Physiology, Institute of Biomembranes, Utrecht University, Utrecht 3584 CH, The Netherlands

Phosphatidic acid (PA) is a minor but important phospholipid that, through specific interactions with proteins, plays a central role in several key cellular processes. The simple yet unique structure of PA, carrying just a phosphomonoester head group, suggests an important role for interactions with the positively charged essential residues in these proteins. We analyzed by solid-state magic angle spinning ^{31}P NMR and molecular dynamics simulations the interaction of low concentrations of PA in model membranes with positively charged side chains of membrane-interacting peptides. Surprisingly, lysine and arginine residues increase the charge of PA, predominantly by forming hydrogen bonds with the phosphate of PA, thereby stabilizing the protein-lipid interaction. Our results demonstrate that this electrostatic/hydrogen bond switch turns the phosphate of PA into an effective and preferred docking site for lysine and arginine residues. In combination with the special packing properties of PA, PA may well be nature's preferred membrane lipid for interfacial insertion of positively charged membrane protein domains.

Phosphatidic acid (PA)[7] is a minor but important bioactive lipid involved in at least three essential and likely interrelated processes in a typical eukaryotic cell. PA is a key intermediate in the biosynthetic route of the main membrane phospholipids and triglycerides (1); it is involved in membrane dynamics, *i.e.* fission and fusion (2–4), and has important signaling functions (5–7). The role of PA in membrane dynamics and signaling is most likely 2-fold, either via an effect on the packing properties of the membrane lipids or via the specific binding of effector proteins (4, 7–9). The origin of the specific binding of effector proteins to PA is not known.

The PA binding domains thus far identified (for review, see Ref. 10) and more recently (7)) are diverse and share no apparent sequence homology, in contrast to other lipid binding domains, such as *e.g.* the PH, PX, FYVE, and C2 domains (11–15). One general feature that the PA binding domains do have in common is the presence of basic amino acids (7). Where examined in detail, these basic amino acids were shown to be essential for the interaction with PA, which underscores the importance of electrostatic interactions. Indeed, the negatively charged phosphomonoester head group of PA would be expected to interact electrostatically with basic amino acids in a lipid binding domain. However, such a simple electrostatic interaction cannot explain the strong preference of PA-binding proteins for PA over other, often more abundant, negatively charged phospholipids.

In a recent study we showed that the phosphomonoester head group of PA has remarkable properties (8). The phosphomonoester head group is able to form an intramolecular hydrogen bond upon initial deprotonation (when its charge is −1), which stabilizes the second proton against dissociation. We provided evidence that competing hydrogen bonds, *e.g.* from the primary amine of the head group of phosphatidylethanolamine (PE), can destabilize this intramolecular hydrogen bond and, thus, favor the further deprotonation, *i.e.* increase the negative charge, of PA (8). These data raised the intriguing hypothesis that a combination of electrostatic and hydrogen bond interactions and not just electrostatic interactions of PA with basic amino acids, *i.e.* lysine and arginine, forms the basis of the (specific) binding of PA to PA-binding proteins.

* The costs of publication of this article were defrayed in part by the payment of page charges. This article must therefore be hereby marked "*advertisement*" in accordance with 18 U.S.C. Section 1734 solely to indicate this fact.

[S] The on-line version of this article (available at http://www.jbc.org) contains supplemental material.

[1] Present address and to whom correspondence should be addressed: Physics Dept., Kent State University, Smith Hall 105, Kent, OH 44242. Tel.: 330-672-7968 or 2246; E-mail: e.e.kooijman@gmail.com.

[2] Supported by Netherlands Organization for Scientific Research/FOM/ALW, "Fysische Biologie" program.

[3] An Alberta Heritage Foundation for Medical Research Senior Scholar and Canadian Institutes of Health Research (CIHR) New Investigator. Work in this group was supported by Natural Science and Engineering Research Council and CIHR.

[4] Supported by Netherlands Organization for Scientific Research, Veni Grant CW 700.52.401 and Vidi Grant CW 700.56.429.

[5] Work in this laboratory was supported by the Netherlands Organization for Scientific Research Grants 813.06.003, 863.04.004, 864.05.001, and 810-36.005 and the Royal Netherlands Academy of Arts and Sciences (KNAW).

[6] Supported by the Human Frontier Science Program Organization and European Community Network Grant HPRN-CT-2002-00259.

[7] The abbreviations used are: PA, phosphatidic acid; PE, phosphatidylethanolamine; PC, phosphatidylcholine; DOPA, 1,2-dioleoyl-*sn*-glycero-3-phosphate (monosodium salt); DOPC, 1,2-dioleoyl-*sn*-glycero-3-phosphocholine; GST, glutathione *S*-transferase; LPA, lysophosphatidic acid; MAS, magic-angle spinning; RPA, Raf-1 PA binding region; MD, molecular dynamics.

We set out to test this hypothesis by determining the ability of lysine and arginine residues in various membrane-interacting polypeptides to form a hydrogen bond with the phosphomonoester head group of PA in a lipid bilayer. Consistent with our hypothesis, we find using magic angle spinning ^{31}P NMR that the positively charged amino acids lysine and arginine in these peptides are able to increase the charge of PA. We conclude that this increase in charge is due to the formation of hydrogen bonds between PA and the basic amino acids. MD simulations provided a dynamic view on the specific docking of these side chains on the di-anionic form of PA. We conclude that the phosphate of PA is an effective and preferred docking site for lysine and arginine residues in membrane-interacting peptides. In combination with its special packing properties, this turns PA into nature's preferred membrane lipid to mediate interfacial insertion of positively charged membrane protein domains. This preference for PA and the role of interfacial insertion was confirmed in binding experiments with the PA binding domain of the protein kinase Raf-1, which is one of the best-characterized PA target proteins (16–19). To conclude, we propose that the electrostatic/hydrogen bond switch provided by the phosphomonoester is a universal mechanism in stabilizing the binding of phosphomonoesters to proteins.

MATERIALS AND METHODS

Sample Preparation—1,2-Dioleoyl-*sn*-glycero-3-phosphate (monosodium salt; DOPA), 1,2-dioleoyl-*sn*-glycero-3-phosphocholine (DOPC), 1,2-dioleoyl-*sn*-glycero-3-phosphoethanolamine (DOPE), and 1,2-dioleoyl-3-trimethylammonium propanediol (chloride salt) were purchased from Avanti Polar lipids (Birmingham, AL). Dimethyldioctadecylammonium (chloride salt) was a kind gift from Dr. M. Scarzello, University of Groningen, The Netherlands. The detergents, dodecylamine and dodecyltrimethylammonium chloride, were purchased from Sigma. Lipid purity was checked by thin layer chromatography and judged to be more than 99% pure. Polyleucine-alanine-based peptides (ALP) (lysine-flanked, KALP; arginine-flanked, RALP; tryptophan-flanked, WALP) were synthesized as described previously and were more than 98% pure as determined by quantitative high performance liquid chromatography (20); poly-L-lysines (hydrobromide) with polymerization degree *n* of 20 and 100 were purchased from Sigma and used without further purification.

Dry lipid films and lipid suspensions were prepared as described previously (8). Lipid/poly-L-lysine samples were prepared by hydrating the lipid film with Hepes buffer (100 mM Hepes, 5 mM acetic acid-NaOH, 100 mM NaCl, and 2 mM EDTA, pH 7.20) containing poly-L-lysine. The resulting lipid/poly-L-lysine dispersions were freeze-thawed at least once, after which the pH of the dispersions was generally found to be within 0.05 pH units of pH 7.20 (if not, the pH was adjusted to fall within this range). The dispersions were centrifuged at 70,000 rpm for 30 min at room temperature in a Beckman TL-100 ultracentrifuge, and the pellet was transferred to 4 mm TiO_2 MAS-NMR sample tubes for ^{31}P NMR measurement. Lipid/polyleucine-alanine peptide films were prepared as described previously (20). These films were hydrated with Hepes buffer, and the dispersions were centrifuged as described above. The clear supernatant was removed, and the pellet was resuspended in Hepes buffer and centrifuged again. This procedure was repeated until the pH of the supernatant was within 0.05 pH units of pH 7.20, after which the samples were freeze-thawed at least once. When the pH of this dispersion was still within 0.05 pH units of pH 7.20, it was centrifuged, and the pellet was transferred to a 4 mm TiO_2 MAS-NMR sample tube; otherwise, the above procedure was repeated until the pH was in the desired range (pH 7.20 $\pm$ 0.05).

NMR Spectroscopy—^{31}P NMR spectra were recorded on a Bruker Avance 500 wide-bore spectrometer (Karlsruhe, Germany) at 202.48 MHz using a 4-mm cross-polarization MAS-NMR probe. Samples were spun at the magic angle (54.7°) at 5 kHz to average the chemical shift anisotropy, and the chemical shift position of PA was recorded relative to 85% H_3PO_4. Under stable spinning conditions typically 500–3000 scans were recorded. Experiments were carried out at a temperature of 20.0 $\pm$ 0.5 °C.

Hydrogen Bond Length Determination—In the Cambridge Structural Data base (version November 2004, with updates of February and May 2005; total number of entries 347767) 395 crystal structure determinations were found containing 1716 fragments that fit the lysine geometry, *i.e.* primary amine-to-phosphate hydrogen bond length (see supplemental Fig. 3*A*). For the arginine geometry, *i.e.* guanidinium-to-phosphate hydrogen bond length (see supplemental Fig. 3*B*), 30 crystal structure determinations were found containing 158 fragments. Searches were performed with the program ConQuest (21); for data analysis the program Vista (22) was used.

MD Simulations—Starting structures for molecular dynamics simulations were based on previous simulations of DOPC-peptide interactions and used the exact same protocols (23). The original DOPC bilayer consists of 64 lipids, 32 in each membrane leaflet. In each leaflet 3 randomly chosen DOPC molecules were changed into DOPA (−1) or DOPA (−2) by removing the choline head group. Head group charges and geometries for DOPA (−1) and DOPA (−2) lipids were calculated using density functional theory calculations and charge-fitting. The resulting charges were close to the phosphate group charges in DOPC.[8] 0.2 M salt was added to match the experimental conditions. The DOPA (−1) simulation system contained 58 DOPC and 6 DOPA (−1) lipids, 2791 water molecules, 11 Na^+ ions, and 5 Cl^- ions. The DOPA (−2) simulation system contained 58 DOPC, 6 DOPA (−2) lipids, 2785 water molecules, 17 Na^+ ions, and 5 Cl^- ions. These two bilayers were simulated for 25 ns for equilibration, as determined by changes in the area per lipid and hydrogen bonding, and 25 ns for production.

Lys_8 and Arg_8 peptides were built in an extended configuration with uncapped termini. Two peptides were added to the water phase of the pre-equilibrated DOPC/DOPA bilayers above by removing overlapping water molecules and adding additional counter ions to maintain a zero net charge in the simulations. Initially the peptides were placed such that they had no contact with lipids at all, but in all cases the peptides rapidly bound at the water/lipid interface and showed little

[8] Z. Xu and D.P. Tieleman, manuscript in preparation.

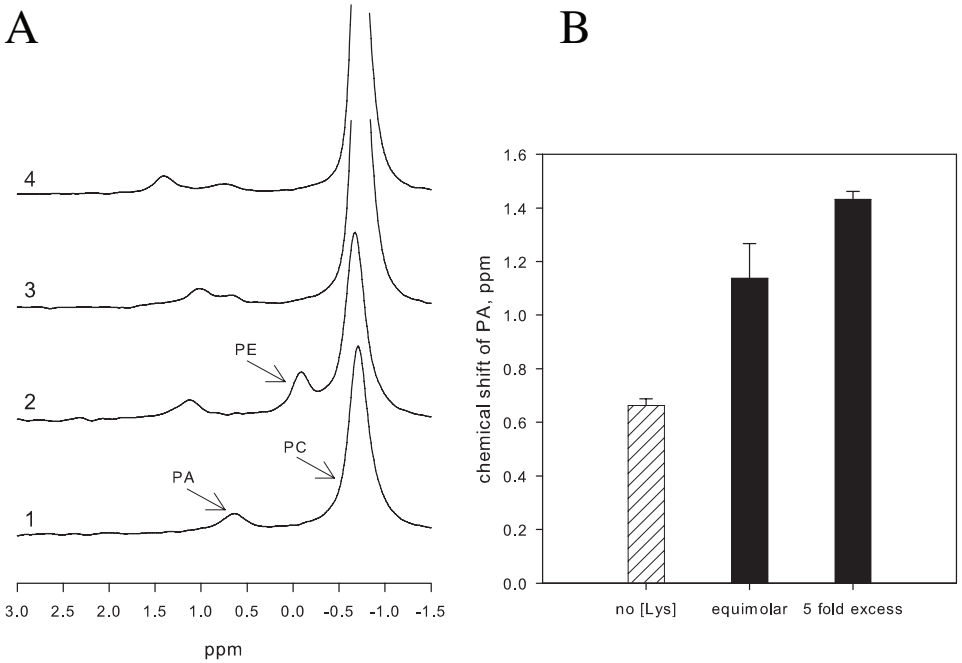

FIGURE 1. *A*, MAS-^{31}P NMR spectra at pH 7.20 for 10 mol % PA in PC (*curve 1*), in PC containing 10 mol % PE (*curve 2*), and in PC hydrated in the presence of poly-L-lysine (Lys_{20}) either equimolar (lysine residues) with respect to PA (*curve 3*) or at a 5-fold molar excess (*curve 4*). The *y* axis for *curves 3* and *4* was amplified (×2) compared with that for *curves 1* and *2*. *B*, quantitation of the effect of poly-L-lysine on the chemical shift of PA in PC/PA (9:1). In this and subsequent figures the *error bar* associated with the control, *i.e.* PC/PA vesicles, corresponds to the S.D. of eight separate experiments, whereas the *error bars* for peptide and amphiphile-containing samples corresponds to the range of at least two individual experiments.

change in depth after the first 10 ns. Equilibration was monitored by following the depth of the center of mass of the peptides in the water/lipid interface and hydrogen bonding between the peptides and lipids. Hydrogen bonding parameters were calculated as averages over the last 10 ns of the 50-ns simulations. For analyses, hydrogen bonds were defined by the geometrical criteria of a donor-acceptor distance of less than 0.35 nm and an acceptor-donor-hydrogen angle of less than 30 degrees. All simulations and analyses were done with GROMACS Version 3.2.1 (24); visualization was done with VMD (25).

Protein Production—A GST fusion of the Raf-1 PA binding region (RPA) (amino acids 390–426) (16) was expressed in *Escherichia coli*. The RPA fragment was amplified by PCR and cloned into the destination vector pDest15 using the Gateway recombination system (Invitrogen). The construct was transformed to *E. coli* strain BL21-AI, and expression was induced by adding arabinose according to the manufacturer's instructions (Invitrogen). Total soluble protein was isolated, and GST-tagged protein was purified using glutathione-Sepharose.

Liposome Binding Assays—Liposome assays were performed as described before (26, 27) with some modifications. Per sample, in total 250 nmol of synthetic dioleoyl phospholipids (all from Avanti Polar Lipids, Alabaster, AL) were mixed at the appropriate molar ratios in chloroform, dried, and subsequently rehydrated in extrusion buffer (250 mM raffinose, 25 mM Tris, pH 7.5, 1 mM dithiothreitol) for 1 h. Unilamellar vesicles were produced using a lipid extruder (0.2-μm filters, Avanti Polar Lipids) according to the manufacturer's instructions. Liposomes were diluted in 3 volumes of binding buffer (125 mM KCl, 25 mM Tris, pH 7.5, 1 mM dithiothreitol, 0.5 mM EDTA) and pelleted by centrifugation at 50,000 × *g* for 15 min. Liposomes were resuspended in binding buffer, added to 300 ng of purified GST-tagged protein, and incubated for 30–45 min in a total volume of 50 μl at room temperature. Liposomes were harvested by centrifugation at 16,000 × *g* for 30 min, washed once in binding buffer, and resuspended in Laemmli sample buffer. Samples were run on SDS-PAGE, and gels were stained with colloidal Coomassie staining (Sigma), scanned, and quantified with ImageQuant (GE Healthcare) before staining with silver.

RESULTS

Basic Amino Acids in Membrane-interacting Peptides Increase the Charge of PA—The ^{31}P chemical shift of PA was previously found to be very sensitive to the ionization (charge) state of the phosphate head group. A change in chemical shift to downfield values, *e.g.* induced by an increase in pH, corresponds to an increase in negative charge observed either via high resolution NMR in small membrane vesicles (28, 29) or by MAS NMR in physiologically more relevant extended bilayers (8). In an earlier study we observed that inclusion of PE in a PA-containing PC bilayer resulted in a profound downfield shift of the ^{31}P NMR peak of PA (8). This is exemplified in Fig. 1*A* (compare *curves 1* and *2*). *Curve 1* shows the MAS ^{31}P NMR spectrum of a PC/PA (9:1) bilayer with the minor downfield peak (to the *left*) corresponding to PA and the major upfield peak (to the *right*) to PC. Inclusion of 10 mol % PE (PC/PE/PA 8:1:1, *curve 2*) results in a large shift of the PA peak to downfield values due to an increase in the charge of PA. This increase in negative charge of PA induced by PE is caused by hydrogen bonding between the primary amine in the head group of PE and the phosphomonoester head group of PA (see (Ref. 8).

To determine whether the basic amino acid lysine, which contains a primary amine, is also able to form a hydrogen bond with PA, we first determined the effect of $polylysine_{20}$ on the chemical shift of PA at neutral pH. $Polylysine_{20}$ with a polymerization degree of 20 was chosen because it binds with high affinity to membranes containing negatively charged phospholipid (30, 31). Fig. 1*A* (*curve 3*) shows that an equimolar amount of lysine residues with respect to PA causes the majority of the PA peak to shift to downfield values. The minor part of the PA peak that does not shift upon polylysine addition most likely represents a small pool of PA in the multilamellar vesicles that is not reached by polylysine. In the presence of an excess of lysine residues with respect to PA (Fig. 1*A*, *curve 4*), maximizing the PA-polylysine interaction, the PA peak shifts even further

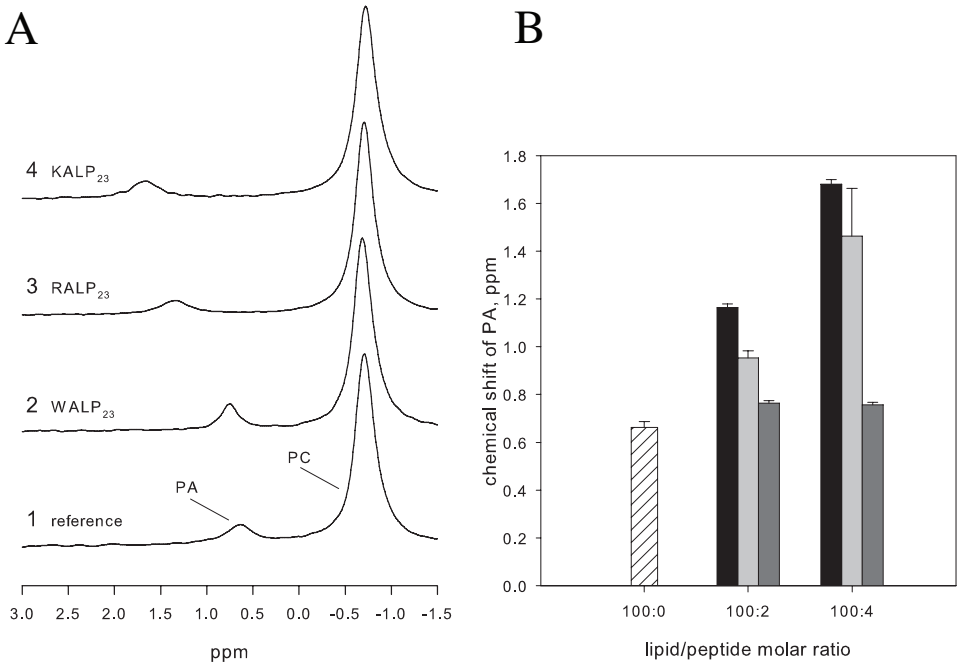

FIGURE 2. *A*, MAS-^{31}P NMR spectra at pH 7.20 for PC/PA (9:1, *curve 1*, same as in Fig. 1) and for PC/PA (9:1) bilayers containing either WALP23 (denotes total number of amino acid residues making up the peptide) (*curve 2*), RALP23 (*curve 3*), or KALP23 (*curve 4*) peptides at a lipid to protein molar ratio of 25:1. *B*, quantification of the chemical shift effects; PC/PA bilayer without peptide (*dashed bar*) and PC/PA bilayer containing KALP23 (*black*), RALP23 (*light gray*), and WALP23 (*dark gray*) at two different lipid to protein ratios.

(see Fig. 1*B* for quantitation). These results were confirmed using another, longer, polylysine (n = 100) (data not shown). Thus, at constant pH, the addition of polylysine results in an increase in the negative charge of PA.

The binding of polylysine to negatively charged lipid membranes is cooperative and requires a polymerization degree of at least five lysine residues (30). In contrast, the PA binding domains that have been identified to date contain a smaller cluster of only 2–4 basic amino acids in their PA binding site (7, 10). To more closely mimic the natural situation, we chose a well characterized experimental system of synthetic polyleucine-alanine α-helical transmembrane peptides flanked on either side by two basic amino acids to study the interaction of small clusters of the basic amino acids, Lys and Arg, with PA (20, 32). Fig. 2*A* shows that at a lipid-to-peptide ratio of 25, KALP23 causes a large downfield shift of the PA peak (quantified in Fig. 2*B*). This demonstrates that KALP23 is indeed able to increase the charge of PA, similar to the effects of PE and polylysine. The effect of KALP23 on the charge of PA depends on the lipid-to-peptide ratio, as is shown in Fig. 2*B* (*black bars*). Identical results were obtained with a KALP31 peptide (data not shown), which has a considerably longer transmembrane segment than the KALP23 peptide (32). RALP23 also causes an increase in the negative charge of PA in the PC/PA bilayer, although slightly less efficient than KALP23 (Fig. 2). As a control we investigated the effect of the tryptophan-flanked peptide WALP23. WALP23 incorporated at different concentrations did not appreciably affect the chemical shift of PA (Fig. 2, *A*, *curve 2*, and *B*), and the considerably longer WALP31 peptide displayed a similar behavior (data not shown). Clearly, the positively charged lysine and arginine residues in KALP and RALP, respectively, are responsible for the observed charge increase of PA and not just the presence of a transmembrane peptide.

The Increase in Charge Is Largely Due to Hydrogen Bonding—Apart from the possibility of forming a hydrogen bond with the phosphomonoester head group of PA, lysine and arginine also introduce a net positive charge at the membrane surface. This will decrease the local proton concentration (due to charge repulsion) and, thus, increase the local (interfacial) pH. An increase in the interfacial pH will result in an increase in the negative charge of PA and is accompanied by a downfield shift of the PA peak. To distinguish between positive charge and hydrogen bond effects, we sought a simpler system in which to address this issue. We chose the positively charged amphiphiles dodecyltrimethylammonium chloride and dodecylamine, since these amphiphiles carry the same positive charge but differ in the ability to form hydrogen bonds because the quaternary amine cannot act as a hydrogen bond donor. Dodecyltrimethylammonium chloride and dodecylamine were included in the PC/PA bilayer at a lipid-to-amphiphile molar ratio of 12.5 and 6.25 to be able to compare the positive charge effects induced by these amphiphiles with those induced by the transmembrane peptides (each KALP and RALP peptide contains 4 positive charges); the results are shown in Fig. 3. As expected, the positively charged dodecyltrimethylammonium chloride increased the charge of PA due to the interaction of a positive charge (Fig. 3, *white bars*; control, *cross-hatched bar*). Similar results were obtained for the structurally very different, quaternary amine containing, diacylamphiphiles, 1,2-dioleoyl-3-trimethylammonium propanediol and dimethyldioctadecylammonium, which also only caused a small increase in the chemical shift and, thus, the negative charge of PA (data not shown). However, dodecylamine, which in addition to being positively charged can also form a hydrogen bond, induced a substantially larger increase in the negative charge of PA (Fig. 3, *striped bars*). Quantitation of the change in charge induced by primary and quaternary amines requires full titration curves, which are shown in supplemental Fig. 1. These data show that at pH 7.2 primary amines induce an ~60% larger increase in the negative charge when compared with quaternary amines. These results clearly demonstrate that hydrogen bond-forming primary amines are able to further increase the negative charge of PA beyond the increase induced by quaternary amines and indicate that the extra increase in negative charge induced by the primary amine is due to the formation of a hydrogen bond with the phosphomonoester head group of PA.

Importantly, the effects induced by the quaternary amines are substantially less than those induced by KALP and RALP

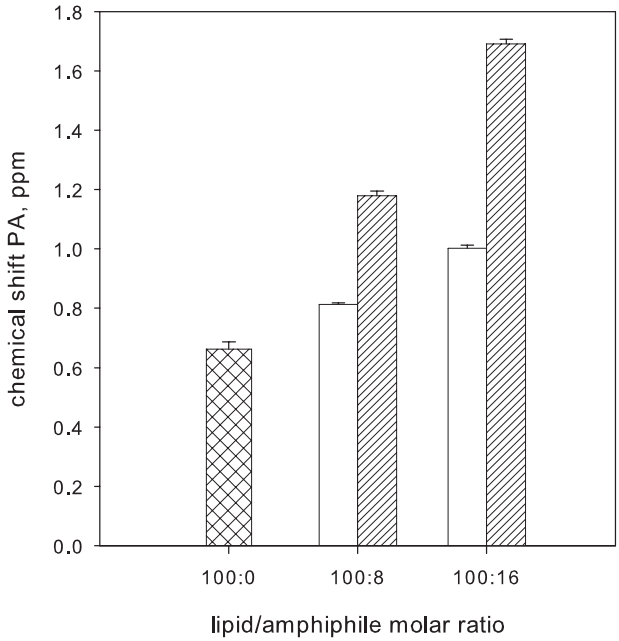

FIGURE 3. **Effects of the amphiphiles dodecyltrimethylammonium (*white bars*) and dodecylamine (*striped bars*) on the chemical shift of PA at two lipid to amphiphile molar ratios; control without amphiphiles (*hatched bar*, identical to that shown in Figs. 1*B* and 2*B*).**

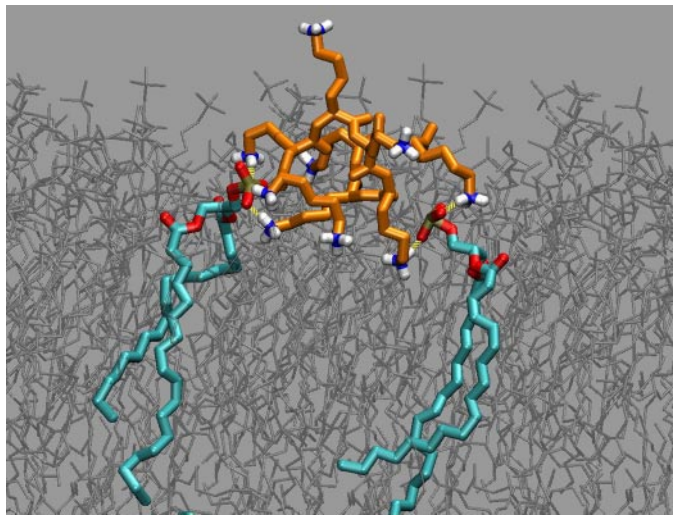

FIGURE 4. **Snapshot of the MD simulation of the PC/PA(−2) bilayer with polylysine$_8$.** PA is shown in *cyan*, with the oxygens in *red*. The polylysine peptide is *orange* with the lysine side chains clearly indicated in *blue* (N)/*white* (H). PC is shown in *gray shading*. Hydrogen bonds between the lysine side chains and the phosphate oxygens of PA are shown in *yellow*.

peptides, whereas the effect of the primary amine dodecylamine is essentially identical to that of KALP (compare Figs. 2*B* and 3). Therefore, we conclude that the interaction of KALP and RALP peptides with PA involves the formation of hydrogen bonds between the basic amino acid residues and the phosphomonoester head group of PA.

Basic Amino Acids Have a Preferential Interaction with Di-anionic PA—To get a broader insight into the interaction of lysine and arginine containing membrane active peptides with a PA-containing PC bilayer, we carried out MD simulations. These simulations were performed with PC bilayers containing 10 mol % of either a mono-anionic or di-anionic PA and contained either polylysine$_8$ or polyarginine$_8$ peptides, one on either side of the lipid bilayer. The length of these peptides is sufficient to assure an efficient interaction with an anionic bilayer (30). The simulations were started with the peptides in solution, and we monitored the interaction between lysine or arginine side chains and phosphates in the head group of PA and PC. The peptides quickly bound to the lipid bilayer (within 10 ns) and stayed bound for the duration of the simulation (50 ns). A two-dimensional snapshot of the simulation of a PC bilayer containing di-anionic-PA in the presence of polylysine$_8$ is shown in Fig. 4. As predicted by the MAS-NMR experiments, hydrogen bond interactions between the di-anionic PA and lysine side chains are clearly visible (*shaded* in *yellow*). However, hydrogen bonds between the phosphate of PC and lysine side chains were also present. To get an estimate of the relative preference of the lysine side chains for a specific lipid (either PA or PC), we determined the total number of hydrogen bonds formed between the peptides and phosphate of mono- and di-anionic PA and PC and compared these to the ratio of PA to PC in the bilayer. The total number of lysine side-chain hydrogen bonds to the phosphate of PA and PC in the simulations containing either mono-anionic or di-anionic PA normalized to the PC/PA ratio in the bilayer are shown in Fig. 5, *A* and *B*, respectively. These normalized histograms show that it is much more likely for a lysine side chain to form a hydrogen bond with the phosphate of di-anionic PA than with the phosphate of PC; in contrast, there is no apparent difference between mono-anionic PA and PC, *i.e.* the histograms overlap. These histograms also indicate that over time PA-2 is clearly accumulated around the polylysine peptide(s), information not readily available from the two-dimensional snapshot of the hydrogen bond interactions of Fig. 4. To provide a visualization of the simulations, a movie of the polylysine, PA-2/PC MD simulation is included in the supplemental information. The hydrogen bond interaction between lysine side chains and di-anionic PA is very stable, with some hydrogen bond lifetimes lasting well over 10 ns (data not shown). Identical simulations were performed with the polyarginine$_8$ peptide, and an identical hydrogen bond analysis was carried out. The normalized histograms for the mono- and di-anionic PA simulations are shown in Fig. 5, *C* and *D*, respectively. These indicate also that arginine side chains are more likely to form a hydrogen bond with the phosphate of di-anionic PA than PC, indicating an accumulation of PA-2 around the polyarginine peptide and that there is no relative preference or accumulation between/around mono-anionic PA and PC.

Binding of a PA Binding Domain Is Enhanced by Negative Membrane Curvature—The unique position of the phosphate head group of PA, very close to the acyl chain region of the lipid bilayer, turns PA into an attractive partner for hydrophobic interactions. Moreover, PA is a type II lipid, *i.e.* has a cone shape (4, 8), and this cone shape of PA will also favor hydrophobic interactions between PA and PA binding domains (33). Indeed, most PA binding domains contain essential hydrophobic residues, typically tryptophans and/or phenylalanines, to allow for such interactions. We investigated the effect of negative curvature on the binding of the well known PA binding domain of the

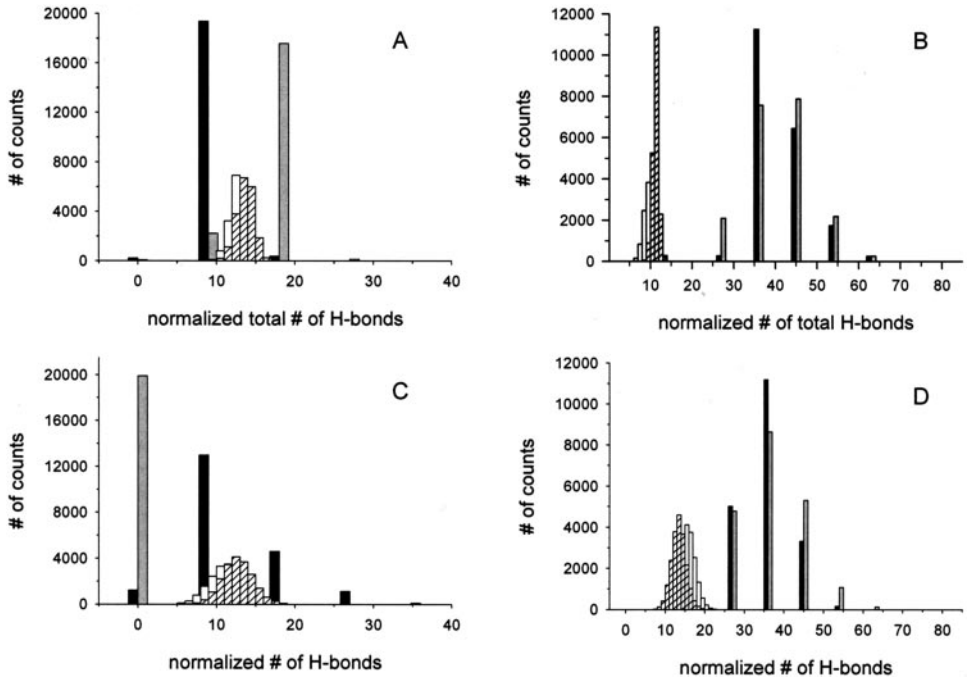

FIGURE 5. **Histograms of the total number of hydrogen bonds between lysine side chains and the phosphate of PC and PA in the DOPC/DOPA(−1)/polylysine$_8$ (*A*) and DOPC/DOPA(−2)/polylysine$_8$ (*B*) simulations and between arginine side chains and the phosphate of PC and PA in the DOPC/DOPA(−1)/polyarginine$_8$ (*C*) and DOPC/DOPA(−2)/polyarginine$_8$ (*D*) simulations, normalized to the PC/PA ratio in the lipid bilayer.** Hydrogen bonds to PC are indicated in *white* and *dashed* (differentiating between the two leaflets of the bilayer) and to PA in *black* and *gray* (differentiating between the two leaflets of the bilayer).

protein kinase Raf-1 (16–19). To this end PC in mixed PC/PA (8:2) model membranes was progressively replaced by PE, and protein binding was monitored. The results (Fig. 6*A*) clearly show that inclusion of PE greatly increases vesicle binding of the Raf-1 PA domain. We not only find, in analogy with literature data, that binding is specific for PA but also that PA specificity is preserved even in the presence of high concentrations of PE (Fig. 6*B*). Similar results were obtained for the plant PA-binding proteins AtPDK1 and AtCTR1.[9]

DISCUSSION

The Phosphomonoester Head Group of PA Is an Effective Docking Site for Basic Amino Acids—We observed that the positively charged amino acids lysine and arginine in the membrane-interacting peptides polylysine, KALP, and RALP caused a downfield shift in the ^{31}P NMR peak of PA at constant pH. We subsequently showed that the main cause behind this increase in negative charge of PA is hydrogen bond formation between the lysine or arginine side chains and the phosphomonoester head group of PA. The existence of hydrogen bonds between the mono- and di-anionic phosphate of PA and lysine and arginine side chains was further confirmed by MD simulation. Interestingly, a similar effect on PA charge is observed irrespective of whether the lysine residues are added from the outside as polylysine or are already stably anchored in the membrane water interface as is the case in the KALP experiments (compare Figs. 1 and 2). The hydrophobic core of the KALP23 (and consequently RALP23 and WALP23) peptide matches the hydrophobic core of the dioleoyllipid bilayer (32) and thereby positions the lysine residues in the acyl chain/head group interface where the phosphate group of PA is located. The position of the phosphate of PA was determined by MD simulation of a peptide free PA/PC (~1:10 molar ratio) bilayer (see "Materials and Methods"). The results indicate that both the monoanionic (PA −1) and di-anionic (PA −2) phosphate of PA is located at the same depth as the phosphates of PC in the head group interface (see supplemental Fig. 2).

Interestingly, the lysine residues in KALP23 and KALP31 induced an identical shift of the PA peak, indicating an equal effect on the negative charge of PA. This is despite the fact that KALP31 is considerably longer than KALP23, with a hydrophobic segment that is ~10 Å longer than the hydrophobic thickness of a DOPC bilayer (32). Earlier studies on KALP peptides in PC bilayers indicate that the lysine residues in KALP are flexibly anchored in the head group region of the lipid bilayer and effectively modulate the hydrophobic length of the peptide to "match" that of the PC bilayer (snorkeling effect, see Ref. 20). Apparently, in the presence of PA, the lysines localize to the PA phosphate instead of throughout the head group region, indicating that the phosphomonoester head group of PA acts as an effective docking site for the lysine residues. Importantly, the formation of hydrogen bonds between lysine residues and PA, as shown by the amphiphile experiments and MD simulation with polylysine$_8$, implies direct docking of the membrane-interacting peptides on the phosphomonoester head group of PA and not merely an electrostatic attraction into the electric layer over the lipid head groups. Furthermore, MD simulation showed that the most effective docking occurs on a di-anionic PA, consistent with our ^{31}P NMR finding that the interaction of lysine residues with the phosphate of PA increases its charge from −1 to −2 at pH 7.2. The interaction between PA and lysine (or arginine) side chains is substantially strengthened by removing a proton (*i.e.* transition from mono- to a di-anionic PA species) from the phosphomonoester head group of PA, which appears energetically favorable in the presence of a positively charged side chain.

Arginine Side Chains Are Weaker Hydrogen Bond Donors than Lysine Side Chains—The increase in PA charge induced by arginine residues in RALP23 is less than that induced by the lysine residues in KALP23. The exact nature of this difference is unclear but may be related to the substantial delocalization of charge in the guanidinium group of arginine when compared with the primary amine of lysine, potentially reducing its hydrogen bond donating capacity. This suggestion is supported

[9] C. Testerink, unpublished data.

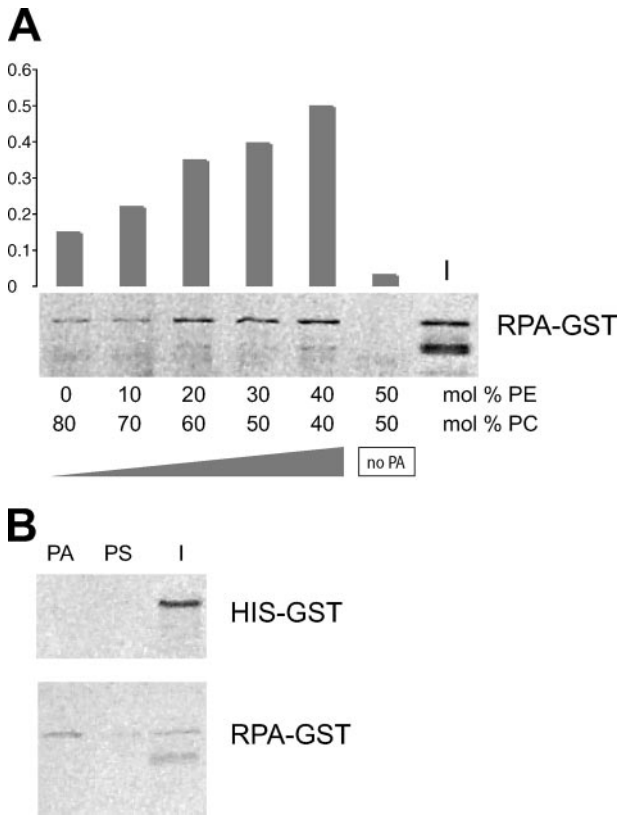

FIGURE 6. **Binding of the RPA to PA-containing liposomes.** Large unilamellar vesicles of different phospholipid composition (250 nmol) were incubated with 300 ng of GST-tagged protein. Bound protein was analyzed on SDS-PAGE and visualized by silver staining. *A*, effect of increasing PE concentration in the liposomes on PA binding. Lipid mixtures consisted of the indicated amounts of PE and PC supplemented with 20% PA, except for the control, an equimolar mixture of PC and PE without PA. *I* is 50% of the input material. *B*, specificity of GST-RPA binding to PA. Lipid mixtures consisted of 40% PC, 40% PE, and 20% PA or 20% phosphatidylserine (*PS*) as indicated. *I* is 50% input. HIS-GST was used as a negative control. The input material shows an additional band underneath RPA-GST, a breakdown product, most likely GST alone, that does not bind to the liposomes.

by a search of the Cambridge Structural data base for the hydrogen bond length of lysine (primary amine)- and arginine (guanidinium group)-like geometries to a phosphate oxygen, which shows that the mean hydrogen bond length for the lysine like compounds (2.813 Å) is ~0.1 Å shorter than that of the arginine-like compounds (2.919 Å, see supplemental Fig. 3). The MD simulations of polylysine$_8$ and polyarginine$_8$ peptides with a PC/PA bilayer further substantiated these results (see supplemental Fig. 4) and showed that indeed the mean hydrogen bond length between arginine and the PA phosphate is ~0.1 Å longer than that for lysine to PA phosphate. These results indicate that indeed the guanidinium group of arginine is a weaker hydrogen bond donor than the primary amine of lysine.

Molecular Model, the Electrostatic/Hydrogen Bond Switch—Collectively our data point to the following mechanism for the interaction of lysine and arginine residues in membrane-interacting peptides with low concentrations of PA (Fig. 7*A*) in a PC bilayer. The positive charge of lysine and arginine side chains in these peptides first results in an electrostatic attraction to the negatively charged phospholipid bilayer. Upon binding to the membrane, the positively charged side chains are able to randomly sample their surroundings, *i.e.* interact electrostatically and form hydrogen bonds with negatively charged (−1) phosphates. However, as soon as the side chain of lysine or arginine encounters the phosphomonoester head group of PA and comes into close enough proximity (<3.5 Å) to form a hydrogen bond, the negative charge of PA increases (to −2) due to the further deprotonation of its phosphomonoester head group. We coin this mechanism the electrostatic/hydrogen bond switch. The increase in negative charge, enhancing the electrostatic attraction, coupled to the formation of hydrogen bonds now locks the positively charged lysine or arginine side chains on the head group of PA and results in a docking of the membrane-interacting peptide on a di-anionic PA molecule. The difference in hydrogen bond length and effect on the negative charge of PA observed between lysine and arginine residues would suggest that lysine residues are more effective in docking on the phosphomonoester head group of PA. We propose that the electrostatic/hydrogen bond switch is a key element of the specific recognition of PA by PA-binding proteins.

Further support for our model comes from the interaction of basic residues in transmembrane proteins with anionic phospholipids and from the interaction of lysophosphatidic acid (LPA) with its G-protein-coupled receptors. An important feature of many transmembrane proteins is that they are flanked on the cytosolic side of the membrane by basic amino acids. These basic residues are thought to stabilize the transmembrane orientation of the protein and/or regulate its activity (34–37). Clusters of these basic amino acids may specifically bind to PA. Indeed, recent evidence suggests that this is the case for the mechanosensitive channel of large conductance MscL. MscL carries a cluster of three basic amino acids (Arg-98, Lys-99, and Lys-100) on its cytosolic face and has a specific, high affinity interaction with PA (38). LPA-like PA has a phosphomonoester head group, and binding of LPA to its G protein-coupled receptors is likely to depend on similar principles as those discussed above for PA. Indeed, the binding of LPA (and coincidentally also its sphingolipid counterpart sphingosine 1-phosphate) to its receptors critically depends on the phosphomonoester head group (39, 40), and the phosphate binding region of the LPA receptors all contain two conserved basic residues (one arginine and one lysine residue (40)). Interestingly, our experimental results and the discussion above would suggest that LPA binds to its receptors in a di-anionic form.

Phosphomonoesters are ubiquitous in nature, occurring not only in lipids such as PA and LPA but also in many proteins, where (de)phosphorylation often switches enzymes between active and nonactive states as well as in many small bioactive molecules, such as glucose 6-phosphate. Recognition and binding to the phosphomonoester moiety(ies) of these compounds is likely regulated by similar principles as those presented for PA (see Fig. 7*A*). Indeed a comparison of the crystal structure of 12 randomly selected proteins binding a phosphomonoester moiety or moieties shows that multiple hydrogen bonds are present between amino acid side chains and the phosphomonoester, which inevitably carries two negative charges (41–53). Lysine and arginine residues form the positively charged binding pocket and often form the hydrogen bond donors as well, but other residues donating side chain hydrogen bonds also

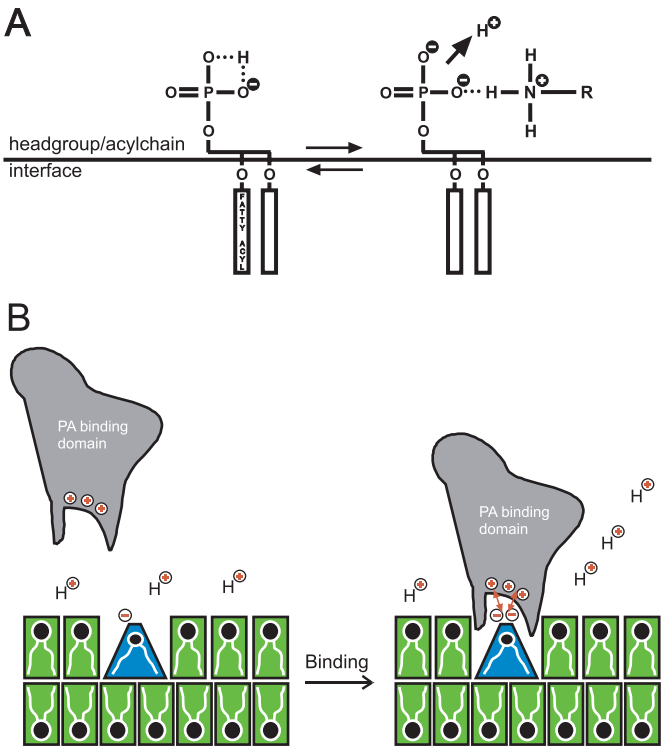

FIGURE 7. *A*, schematic representation of the proposed electrostatic/hydrogen bond switch model for the increase in negative charge of PA induced by positively charged amino acid residues. Positive charge and hydrogen bond formation is shown for the primary amine of a lysine residue, but can in principle be any combination of positively charged ion and hydrogen bond donor. Intra- and intermolecular hydrogen bond interactions are indicated by a *dotted line*. The location of the intermolecular hydrogen bond between PA and the primary amine of a lysine residue shown in the figure is only indicative. *B*, model for the interaction of positively charged protein domains with PA. The molecular shape of PA (a cone shaped lipid) is shown schematically as is the location of the head group of PA deep into the lipid head group region of a PC bilayer. The electrostatic/hydrogen bond switch is incorporated in this model.

regularly occur. We propose that the electrostatic/hydrogen bond switch is the mechanism by which phosphomonoesters are recognized and bound by proteins.

PA Is the Preferred Anionic Lipid for the Interfacial Insertion of Proteins—The docking of basic protein domains on PA may be followed by insertion of hydrophobic protein domains into the hydrophobic interior of the lipid bilayer (see Fig. 7*B*). One example of such a favorable hydrophobic interaction has been described *in vitro* for the GTPase dynamin. Dynamin, which binds to negatively charged membranes, shows considerably more insertion in mixed-lipid monolayers containing PA instead of other negatively charged phospholipids (the molecular area of insertion is highest in the presence of PA; see Ref. 54). How can we understand these hydrophobic interactions? On top of its high charge and capacity to form hydrogen bonds, (unsaturated) PA also has a special molecular shape (Refs. 4 and 9; see Fig. 6*B*). PA is the only anionic phospholipid with a pronounced cone shape under physiological conditions (37). Cone-shaped lipids facilitate protein penetration into the membrane by forming favorable insertion sites in the head group region of the lipid bilayer (33). We further confirmed the effect of cone shape lipids on the binding of PA binding proteins to PA in experiments with the well known PA binding domain of the protein kinase Raf-1 (RPA). The cone-shaped lipid PE was found to strongly increase PA binding of the PA binding domain of Raf-1. This binding depended critically on the presence of PA. Only hydrophobic insertion sites did not lead to a binding of the RPA domain, and RPA bound at least 2.5-fold more to PA when compared with phosphatidylserine, even in the presence of high concentrations of PE.

Our observation that PA may act as a docking site for membrane-interacting peptides very close to the hydrophobic interior of the lipid bilayer together with the cone shape of PA turns PA into a very effective insertion site for positively charged membrane-active proteins. We propose that the electrostatic/hydrogen bond switch in the phosphate head group of PA coupled to the location of the phosphate head group close to the hydrophobic interior of the lipid bilayer sets PA apart from all the other anionic membrane lipids.

Acknowledgments—We thank Antoinette Killian and Rob Liskamp for helpful discussions and suggestions on the use and properties of the polyleucine-alanine peptides. Huub Kooijman is acknowledged for expert advice on the Cambridge structural data base.

Note Added in Proof—A recent MD study of the potassium channel KcsA has shown that PA binds and forms extensive hydrogen bonds between its phosphomonoester headgroup and two conserved arginine residues in the interface between the monomers making up the KcsA tetramer (55). Consistent with this observation PA was found to strongly and specifically stabilize the tetramer against tetrafluoroethanol (TFE) induced dissociation (M. Raja, R. E. Spelbrink, B. de Kruijff, and J. A. Killian, unpublished observations).

REFERENCES

1. Athenstaedt, K., and Daum, G. (1999) *Eur. J. Biochem.* **266,** 1–16
2. Ktistakis, N. T., Brown, H. A., Waters, M. G., Sternweis, P. C., and Roth, M. G. (1996) *J. Cell Biol.* **134,** 295–306
3. Chen, Y. G., Siddhanta, A., Austin, C. D., Hammond, S. M., Sung, T. C., Frohman, M. A., Morris, A. J., and Shields, D. (1997) *J. Cell Biol.* **138,** 495–504
4. Kooijman, E. E., Chupin, V., de Kruijff, B., and Burger, K. N. J. (2003) *Traffic* **4,** 162–174
5. English, D., Cui, Y., and Siddiqui, R. A. (1996) *Chem. Phys. Lipids* **80,** 117–132
6. Freyberg, Z., Siddhanta, A., and Shields, D. (2003) *Trends Cell Biol.* **13,** 540–546
7. Testerink, C., and Munnik, T. (2005) *Trends Plant Sci.* **10,** 368–375
8. Kooijman, E. E., Carter, K. M., van Laar, E. G., Chupin, V., Burger, K. N., and de Kruijff, B. (2005) *Biochemistry* **44,** 17007–17015
9. Kooijman, E. E., Chupin, V., Fuller, N. L., Kozlov, M. M., de Kruijff, B., Burger, K. N. J., and Rand, P. R. (2005) *Biochemistry* **44,** 2097–2102
10. Andresen, B. T., Rizzo, M. A., Shome, K., and Romero, G. (2002) *FEBS Lett.* **531,** 65–68
11. Rizo, J., and Sudhof, T. C. (1998) *J. Biol. Chem.* **273,** 15879–15882
12. Maffucci, T., and Falasca, M. (2001) *FEBS Lett.* **506,** 173–179
13. Ellson, C. D., Andrews, S., Stephens, L. R., and Hawkins, P. T. (2002) *J. Cell Sci.* **115,** 1099–1105
14. Stenmark, H., Aasland, R., and Driscoll, P. C. (2002) *FEBS Lett.* **513,** 77–84
15. Lemmon, M. A. (2003) *Traffic* **4,** 201–213
16. Ghosh, S., Strum, J. C., Sciorra, V. A., Daniel, L., and Bell, R. M. (1996) *J. Biol. Chem.* **271,** 8472–8480
17. Rizzo, M. A., Shome, K., Vasudevan, C., Stolz, D. B., Sung, T. C., Frohman, M. A., Watkins, S. C., and Romero, G. (1999) *J. Biol. Chem.* **274,** 1131–1139
18. Rizzo, M. A., Shome, K., Watkins, S. C., and Romero, G. (2000) *J. Biol.*

Chem. **275,** 23911–23918
19. Ghosh, S., Moore, S., Bell, R. M., and Dush, M. (2003) *J. Biol. Chem.* **278,** 45690–45696
20. de Planque, M. R., Boots, J. W., Rijkers, D. T., Liskamp, R. M., Greathouse, D. V., and Killian, J. A. (2002) *Biochemistry* **41,** 8396–8404
21. Bruno, I. J., Cole, J. C., Edgington, P. R., Kessler, M., Macrae, C. F., McCabe, P., Pearson, J., and Taylor, R. (2002) *Acta Crystallogr. B* **58,** 389–397
22. CCDC (1994) *Vista: A Program for the Analysis and Display of Data Retrieved from the CSD*, Cambridge Crystallographic Data Centre, Cambridge, England
23. Aliste, M. P., MacCallum, J. L., and Tieleman, D. P. (2003) *Biochemistry* **42,** 8976–8987
24. Lindahl, E., Hess, B., and van der Spoel, D. (2001) *J. Mol. Model.* **7,** 306–317
25. Humphrey, W., Dalke, A., and Schulten, K. (1996) *J. Mol. Graph.* **14,** 33–38
26. Levine, T. P., and Munro, S. (2002) *Curr. Biol.* **12,** 695–704
27. Loewen, C. J., Gaspar, M. L., Jesch, S. A., Delon, C., Ktistakis, N. T., Henry, S. A., and Levine, T. P. (2004) *Science* **304,** 1644–1647
28. Koter, M., de Kruijff, B., and van Deenen, L. L. (1978) *Biochim. Biophys. Acta* **514,** 255–263
29. Hauser, H. (1989) *Proc. Natl. Acad. Sci. U. S. A.* **86,** 5351–5355
30. de Kruijff, B., Rietveld, A., Telders, N., and Vaandrager, B. (1985) *Biochim. Biophys. Acta* **820,** 295–304
31. Kim, J., Mosior, M., Chung, L. A., Wu, H., and McLaughlin, S. (1991) *Biophys. J.* **60,** 135–148
32. de Planque, M. R., Goormaghtigh, E., Greathouse, D. V., Koeppe, R. E., 2nd, Kruijtzer, J. A., Liskamp, R. M., de Kruijff, B., and Killian, J. A. (2001) *Biochemistry* **40,** 5000–5010
33. van den Brink-van der Laan, E., Killian, J. A., and de Kruijff, B. (2004) *Biochim. Biophys. Acta* **1666,** 275–288
34. van Klompenburg, W., Nilsson, I., von Heijne, G., and de Kruijff, B. (1997) *EMBO J.* **16,** 4261–4266
35. Killian, J. A., and von Heijne, G. (2000) *Trends Biochem. Sci.* **25,** 429–434
36. Lee, A. G. (2004) *Biochim. Biophys. Acta* **1666,** 62–87
37. Zimmerberg, J., and Kozlov, M. M. (2005) *Nat. Rev. Mol. Cell Biol.* **7,** 9–19
38. Powl, A. M., East, J. M., and Lee, A. G. (2005) *Biochemistry* **44,** 5873–5883
39. Lynch, K. R., and Macdonald, T. L. (2002) *Biochim. Biophys. Acta* **1582,** 289–294
40. Sardar, V. M., Bautista, D. L., Fischer, D. J., Yokoyama, K., Nusser, N., Virag, T., Wang, D. A., Baker, D. L., Tigyi, G., and Parrill, A. L. (2002) *Biochim. Biophys. Acta* **1582,** 309–317
41. Oliva, G., Fontes, M. R., Garratt, R. C., Altamirano, M. M., Calcagno, M. L., and Horjales, E. (1995) *Structure* **3,** 1323–1332
42. Aleshin, A. E., Zeng, C., Bourenkov, G. P., Bartunik, H. D., Fromm, H. J., and Honzatko, R. B. (1998) *Structure* **6,** 39–50
43. Baraldi, E., Carugo, K. D., Hyvonen, M., Surdo, P. L., Riley, A. M., Potter, B. V., O'Brien, R., Ladbury, J. E., and Saraste, M. (1999) *Structure* **7,** 449–460
44. Ferguson, K. M., Kavran, J. M., Sankaran, V. G., Fournier, E., Isakoff, S. J., Skolnik, E. Y., and Lemmon, M. A. (2000) *Mol. Cell* **6,** 373–384
45. Lietzke, S. E., Bose, S., Cronin, T., Klarlund, J., Chawla, A., Czech, M. P., and Lambright, D. G. (2000) *Mol. Cell* **6,** 385–394
46. Bravo, J., Karathanassis, D., Pacold, C. M., Pacold, M. E., Ellson, C. D., Anderson, K. E., Butler, P. J., Lavenir, I., Perisic, O., Hawkins, P. T., Stephens, L., and Williams, R. L. (2001) *Mol. Cell* **8,** 829–839
47. Dumas, J. J., Merithew, E., Sudharshan, E., Rajamani, D., Hayes, S., Lawe, D., Corvera, S., and Lambright, D. G. (2001) *Mol. Cell* **8,** 947–958
48. Kutateladze, T., and Overduin, M. (2001) *Science* **291,** 1793–1796
49. Thomas, C. C., Deak, M., Alessi, D. R., and van Aalten, D. M. (2002) *Curr. Biol.* **12,** 1256–1262
50. Lee, D. C., Cottrill, M. A., Forsberg, C. W., and Jia, Z. (2003) *J. Biol. Chem.* **278,** 31412–31418
51. Graham Solomons, J. T., Zimmerly, E. M., Burns, S., Krishnamurthy, N., Swan, M. K., Krings, S., Muirhead, H., Chirgwin, J., and Davies, C. (2004) *J. Mol. Biol.* **342,** 847–860
52. Lee, J. H., and Jeffery, C. J. (2005) *Protein Sci.* **14,** 727–734
53. Lee, S. A., Eyeson, R., Cheever, M. L., Geng, J., Verkhusha, V. V., Burd, C., Overduin, M., and Kutateladze, T. G. (2005) *Proc. Natl. Acad. Sci. U. S. A.* **102,** 13052–13057
54. Burger, K. N. J., Demel, R. A., Schmid, S. L., and de Kruijff, B. (2000) *Biochemistry* **39,** 12485–12493
55. Deol, S. S., Domene, C., Bond, P. J., and Sansom, M. S. P. (2006) *Biophys. J.* **90,** 822–830

Supplementary material:

Quantitation of changes in PA charge: positive charge and H-bond interactions

The interaction of positive charge and hydrogen bonds with the phosphomonoester headgroup of PA increases its negative charge. Both effects could be discriminated by the use of simple quaternary- (positive charge only) and primary- (identical positive charge and H-bond donor) amine containing amphiphiles. From changes in the chemical shift of PA induced by these amphiphiles it was clear that hydrogen bond formation increases the negative charge of PA over that induced by the interaction of a positive charge only. However, these results did not quantify this effect in terms of actual changes in negative charge (i.e. changes in pK_{a2}).

Therefore, pH titration curves, shown in Figure A1, were constructed according to previously established procedures (1). KALP23, containing 4 lysine residues, was chosen as the primary amine containing compound, whereas DOTAP was chosen as the quaternary amine containing compound. The control, 10 mol% PA in 90 mol% PC was taken from (1). The pK_{a2} of PA changed from 7.92 ± 0.03 for the PC/PA (9:1) bilayer, to 7.55 ± 0.03 for the PC/PA (9:1) bilayer containing DOTAP at a lipid to DOTAP molar ratio of 6.25, to 7.16 ± 0.05 for the PC/PA (9:1) bilayer containing KALP23 at a lipid to KALP23 molar ratio of 25 (i.e. a lysine to lipid ratio of 6.25). At pH 7.2, indicated in the figure by the vertical line, this corresponds to the following changes in the negative charge of PA: 1.16 e (negative charge unit), to 1.32 e to 1.54 e for the control, DOTAP and KALP23 containing bilayers respectively. These results indicate that primary amines increase the negative charge of PA by ~60% more than quaternary amines and thus confirm the dominant role of hydrogen bonds in the increase in negative charge of PA by membrane interacting peptides containing the basic amino acids lysine and arginine.

Mean H-bond length of lysine-to-phosphate- and arginine-to-phosphate-like geometries

Lysine and arginine, in KALP23 and RALP23, respectively increase the negative charge of PA in a PC/PA (9:1) bilayer. However, the increase induced by RALP23 is less than that induced by KALP23. This is despite their identical positive charge and ability to form a hydrogen bond with the phosphomonoester headgroup of PA.

One suggestion that would explain the smaller effect of RALP23 on the negative charge of PA is that arginine is a weaker side chain hydrogen bond donor than lysine. In order to investigate this hypothesis we searched the Cambridge Structural database for the mean hydrogen bond length, which is a measure of hydrogen bond strength, of lysine-to-phosphate- and arginine-to-phosphate-like geometries. These geometries are shown in Figure A2 A and B respectively.

The resulting histograms are shown in Figure A2, A and B for the lysine and arginine geometry respectively. From these data the mean hydrogen bond length found for “lysine” was 2.813 Å and for “arginine” 2.919 Å, clearly indicating that lysine residues are likely to be stronger side chain hydrogen bond donors than arginine residues.

Reference:

1. Kooijman, E.E., Carter, K.M., van Laar, E.G., Chupin, V., Burger, K.N.J., de Kruijff B, (2005) *Biochemistry* **44**, 17007-17015

Supplementary Figure Legends:

Supplementary Figure 1: pH titration curves for PA in PC/PA (9:1, molar ratio) bilayers containing KALP23 (squares) at a lipid to KALP23 molar ratio of 25, DOTAP (triangles) at a lipid to DOTAP molar ratio of 6.25. The control (circles) is also shown, taken from (1). The arrows emphasize the differences in charge at pH 7.2.

Supplementary Figure 2: Distribution of phosphate groups across the lipid bilayer determined from MD simulations of DOPC/DOPA(2-) and DOPC/DOPA(1-) lipid bilayers. Phosphates of PC are colored red whereas those of PA are colored green. Also indicated in this figure is the overall system density as it changes across the bilayer and the distribution of solvent (H_2O).

Supplementary Figure 3: Histograms of the N…O hydrogen bond length in Ångstrom for *A*, lysine-to-phosphate-like geometries, and *B*, arginine-to-phosphate-like geometries. The hydrogen bond is indicated by the dotted line between the nitrogen and oxygen atom. Data were compiled using the Cambridge Structural database as described in the Materials and Methods.

Supplementary Figure 4: Hydrogen-bond length distribution between lysine side chains and the phosphate of PA (green and blue, both sides of the bilayer) and arginine side chains and the phosphate of PA (red and black, both sides of the bilayer) taken over the last 10 ns of the 50 ns simulation. Only data from the simulations involving a doubly charged PA (thus PA(2-)) are shown since this situation is most relevant to the comparison with the ^{31}P NMR data.

Supplementary Movie Caption:

Supplementary Movie 1: Animation of 50 ns simulation of the Lys_8 peptide in a DOPA(2-)/DOPC mixture. The two peptides are shown in spacefilling representation. The 6 DOPA (2-) lipids are shown in yellow. Choline nitrogen atoms are blue, lipid oxygen atoms red. Chloride ions are shown as purple spheres, sodium ions as silver spheres. The simulation cell is periodic: molecules leaving on the left enter on the right and vice versa.

Supplementary Figure 1

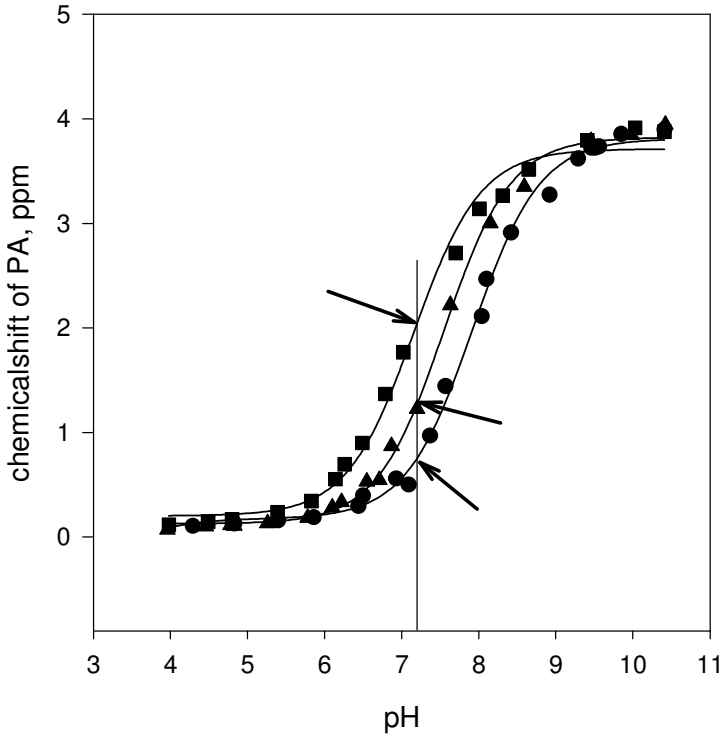

Supplementary Figure 2

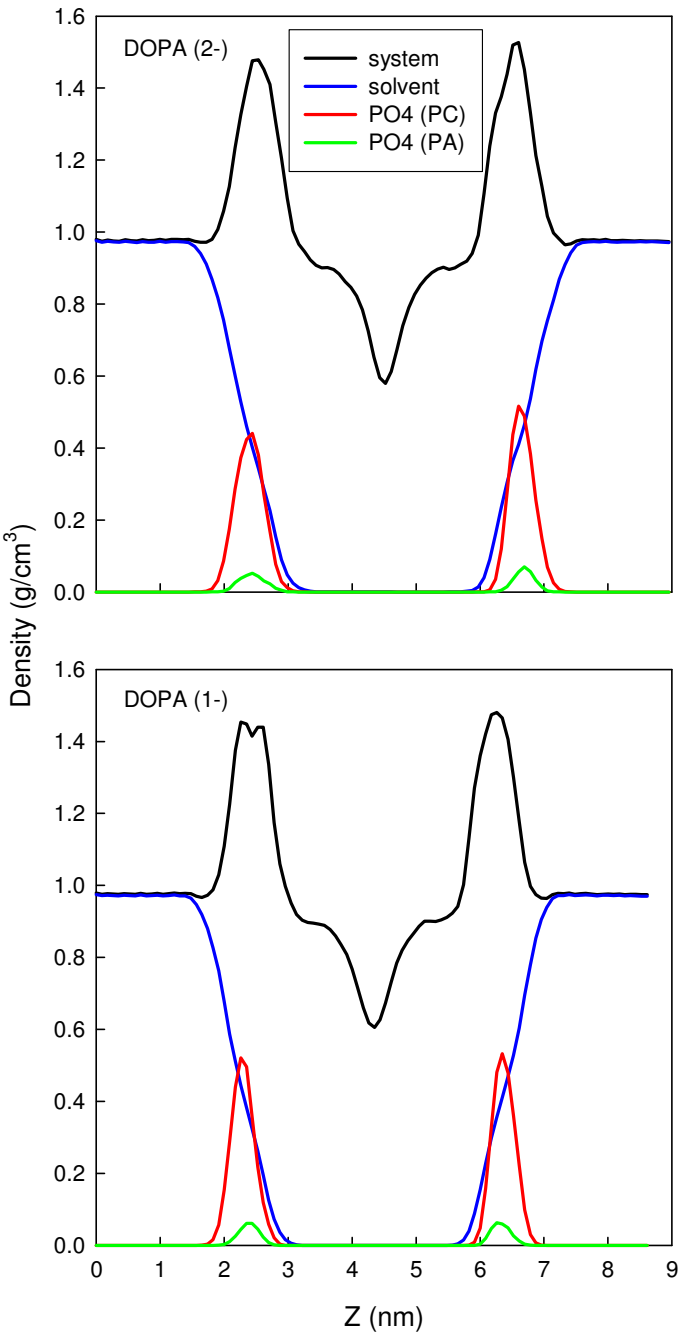

Supplementary Figure 3

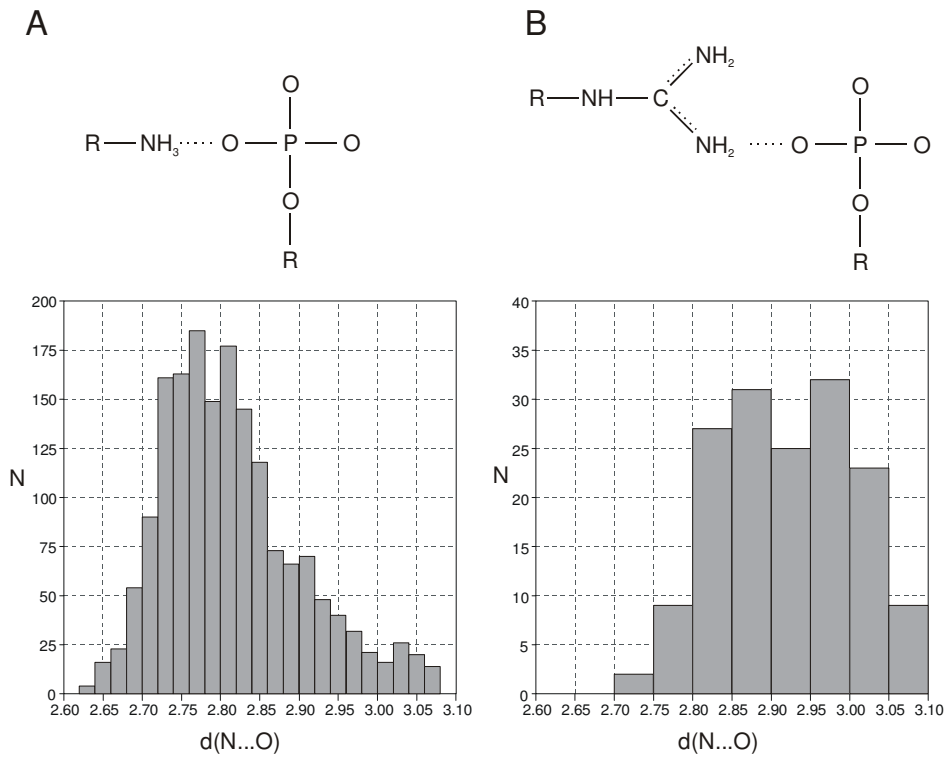

Supplementary Figure 4